Adaptive Control of a Farm Tractor with Varying Yaw Dynamics Accounting for Actuator Dynamics and Saturations

J. Benton Derrick , David M. Bevly

Department of Mechanical Engineering
Auburn University, AL 36849
Email: {derrijb, dmbevly}@auburn.edu

***Abstract*— This paper presents an adaptive control system implemented on an automatically steered farm tractor. The yaw dynamics of the tractor are time varying due to different attached implements and soil conditions; therefore, a model reference adaptive control (MRAC) system is developed to automatically adjust the feed-forward yaw rate controller to changes in the current yaw plant. The MRAC algorithm is next modified from it's original form to account for steering actuator dynamics and nonlinearities. Simulated results are presented that demonstrate the algorithm's performance under ideal conditions. Experimental results are presented that show that the algorithm performs well on a real system with changing yaw dynamics. Finally, experimental results are shown that demonstrate improved tracking performance verses a fixed-gain configuration.**

Fig. 1. John Deere 8420 Equipped with Starfire DGPS and AutoTrac Technology

I. INTRODUCTION

Farm tractors are good candidates for being automatically steered since many maneuvers are continually repeated on land with good Global Positioning System (GPS) satellite visibility. Poor driver visibility, inexperience, fatigue, and overlap are just some of the problems that can be addressed with automatic steering systems. A John Deere 8420 production model outfitted with a StarFire differential GPS system and AutoTrac technology is shown in Fig. 1. This tractor is able to track straight paths with no driver input at the steering wheel.

Farm tractors can be configured with a myriad of implement configurations and encounter various soil conditions. These variations inflict a wide range of lateral hitch forces. It has been previously shown that not taking this variation into account can cause instability [1]. Crop destruction and uneven application can occur with a poorly tuned controller. Therefore, a fixed-gain compensator is not sufficient for all configurations.

There have been past studies that try to adapt the steering controller to account for lateral hitch force variability; most have tried an indirect adaptation technique. A method of estimating yaw model parameters on-line using a variety of estimation techniques such as least mean squares and the extended Kalman filter has been developed [2]. It has been determined that the DC gain of the steering angle to yaw rate transfer function is the parameter that fluctuates the most with respect to hitch loading [1]. Consequently, a method has been developed to estimate the DC gain of the yaw rate transfer function. Once the DC gain is known, a look-up table is used to schedule the controller values.

Currently, the production model tractors have a sensitivity gain that has to be adjusted by the user for different implements. This is not an ideal solution because soil conditions often change from one end of the field to the other. Also, the sensitivity gain does not change when the implement is out of the ground. This often makes the tractor behave erratically when crossing waterways with heavy implements. It is desired that this gain be adjusted on-line so the controller performance will be more robust to different situations. Therefore, this paper will present a direct method for adjusting the sensitivity gain using a model-reference adaptive control (MRAC) system.

Adaptive control techniques are advantageous because they adjust parameters so that the closed-loop performance converges with a desired closed-loop configuration [3]. Previous studies have been completed on MRAC of yaw dynamics in the presence of active steering [4]. Also, vehicle guidance has been adapted using a form of MRAC [5]. A gain schedule approach to active steering of a ground vehicle has been developed using a form of the bicycle model [6].

A dynamic yaw model has been developed that accounts for the change in lateral hitch force [7]. A cascaded controller is used to regulate the lateral position of the tractor. Steering angle, yaw rate, and lateral position are fed back and individually controlled. Since only the yaw rate dynamics change with respect to hitch loading, only the yaw rate controller will be adapted. The adaptation algorithm is then augmented to handle the inner-loop actuator dynamics and saturations. Finally, simulated and experimental results are presented.

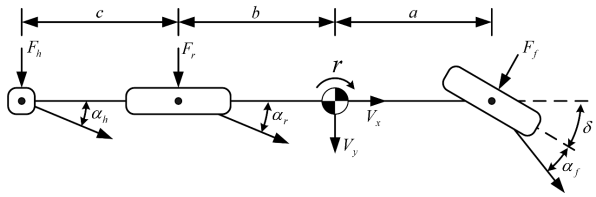

Fig. 2. Bicycle Model with Augmented Lateral Hitch Force

II. Model and Control Structure

A. Tractor Dynamic Yaw Model

Previous studies have been done on modeling the effects of lateral hitch forces on yaw rate dynamics. One study proposed a model in which the implement is modeled as a third axle behind the tractor [7]. Another study has shown this model's validity through experimentation for implements attached to the three-point hitch [8].

The bicycle model of a vehicle lumps the inner and outer wheels of each axle into a single wheel. Therefore, the model inherently neglects weight transfer between the inner and outer wheels. A schematic of the tractor modeled as a bicycle is shown in Fig. 2. Notice that the hitch force is modeled as an extra axle behind the rear axle. The lateral tire force at each axle (F_f, F_r, F_h) is a function of the slip angles $(\alpha_f, \alpha_r, \alpha_h)$ at each axle [9]. The slip angle is defined as the angle between the velocity vector and the heading of each axle. The linearized bicycle model assumes the steering and slip angles are small, and the lateral tire force is proportional to the slip angles at the respective axle. The proportionality constant is called the cornering stiffness and is denoted by $C_{\alpha f}, C_{\alpha r}, C_{\alpha h}$. The hitch cornering stiffness, $C_{\alpha h}$, is the parameter that changes with different implements. The lengths from the center of gravity to the front and rear axle are a and b, and the length from the rear axle to the hitch is c. The variables V_y and V_x are the lateral and longitudinal velocities, and δ is the steering angle of the front axis. The transfer function from steering angle to yaw rate (r) is shown in (1).

$$
\begin{aligned}
&G_{Pr} = \tfrac{r(s)}{\delta(s)} = \tfrac{n_1 \cdot s + n_0}{d_2 \cdot s^2 + d_1 \cdot s + d_0} \\
&n_0 = \tfrac{C_{\alpha f} C_1 + a C_{\alpha f} C_2}{m V_x} \\
&n_1 = a C_{\alpha f} \\
&d_0 = \tfrac{C_2 C_3 - C_1^2}{m V_x^2} + C_1 \\
&d_1 = \tfrac{C_2 I_{zz}}{m V_x} + \tfrac{C_3}{V_x} \\
&d_2 = I_{zz} \\
&C_1 = ((b+c) \cdot C_{\alpha h} + b \cdot C_{\alpha r} - a \cdot C_{\alpha f}) \\
&C_2 = (C_{\alpha h} + C_{\alpha r} + C_{\alpha f}) \\
&C_3 = ((b+c)^2 C_{\alpha h} + b^2 C_{\alpha r} + a^2 C_{\alpha f})
\end{aligned}
\tag{1}
$$

A kinematic relationship between yaw rate and lateral position is used as the lateral position plant model. Lateral position (y) can be described by (2) where β is the side slip angle at the center of gravity, ν is the angle of the velocity vector with respect to the desired longitudinal direction, and V is the magnitude of velocity.

$$
\begin{aligned}
\dot{y} &= V \sin(\nu) \\
\dot{\nu} &= r + \dot{\beta}
\end{aligned}
\tag{2}
$$

Linearizing assuming small angles yields the transfer function from yaw rate to lateral position shown in (3).

$$
G_{Py} = \frac{y(s)}{r(s)} = \frac{V}{s^2} \tag{3}
$$

B. Control Structure

A set of cascaded controllers is used to regulate the lateral position of the tractor. Three feedback loops are implemented using the measurements of the steering angle sensor (δ), yaw rate gyroscope (r), and GPS receiver (y). A schematic of the controller system is shown in Fig. 3. The lateral position, yaw rate, and steering angle controllers are labeled as G_{Cy}, G_{Cr}, and $G_{C\delta}$. The block labeled $G_{Cr_{ff}}$ is the feed-forward yaw rate controller. The steering servo, yaw rate, and lateral position plants are labeled G_{Py}, G_{Pr}, and $G_{P\delta}$.

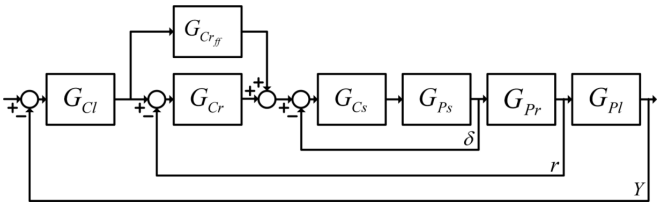

Fig. 3. Cascaded Control Block Diagram

The steering controller was chosen to have a proportional control law with the coefficient of $k_{p\delta}$ shown in (4).

$$
G_{C\delta} = \frac{\delta_{input}(s)}{\delta_{err}(s)} = k_{p\delta} \tag{4}
$$

A proportional controller was chosen because the servo is well-damped and has a pure integrator.

The yaw rate controller was chosen to have a proportional feedback and a proportional feed-forward control law. The feedback coefficient is k_{pr} and the feed-forward coefficient is k_{ff} times the adaptation gain K. The coefficient k_{ff} is equal to the inverse of the DC gain of the steering angle to yaw rate transfer function. The DC gain is the parameter that changes most with hitch loading, hence the reason for the adaptation gain multiplier. The feedback control equation is shown in (5).

$$
G_{Cr} = \frac{\delta_{des_{fb}}(s)}{r_{err}(s)} = k_{pr} \tag{5}
$$

The feed-forward control equation is shown in (6).

$$
G_{Cr_{ff}} = \frac{\delta_{des_{ff}}(s)}{r_{des}(s)} = k_{ff} K \tag{6}
$$

The desired steering angle from the yaw rate controller is then determined by adding the desired steering angle

from the feedback and feed-forward controllers. This is represented in (7).

$$\delta_{des}(s) = \delta_{des_{fb}}(s) + \delta_{des_{ff}}(s) \tag{7}$$

The lateral position controller is a proportional-integral-derivative (PID) control law. The proportional coefficient is k_{py}, the integral coefficient is k_{iy}, and the derivative coefficient is k_{dy}. The equation for the controller is shown in (8).

$$G_{Cy} = \frac{r_{des}(s)}{y_{err}(s)} = k_{py} + \frac{k_{iy}}{s} + k_{dy} \cdot s \tag{8}$$

This control law was selected to add damping to the lateral position response and to offset any steady-state lateral position error.

In this paper, velocity is held constant in all simulations and experiments. Therefore, the controllers of the inner steering loop and outer lateral position loop will remain in fixed-gain configurations. The yaw rate controller will be adapted to offset any changes in the lateral hitch force by adapting the feed-forward gain by the scaling K.

III. MRAC Algorithm

It has be shown experimentally that the DC gain of the steering angle to yaw rate transfer function is the model parameter that changes the most with hitch loading [1]. The assumption is now made that the effects on the pole-zero locations with respect to the $C_{\alpha h}$ parameter is negligible.

In steady-state conditions, the difference in the yaw rate of the tractor with different lateral hitch forces is the DC gain. If the yaw rate of the tractor is desired to be equal for all implements, the desired steering angle needs to scaled accordingly. It can be noted that scaling the feed-forward gain will accomplish this goal.

For this paper, the MIT rule gradient technique is used to derive the the feed-forward control update law. The MIT rule is the original approach to MRAC [3]. The drawback to this method is that general stability cannot be proven. Stability of linear time invariant systems using the MIT rule has been proven under certain circumstances [10], but this technique will not work for the system at hand since the changing hitch loading causes the dynamics to be time varying.

A schematic of the adaptive scheme is shown in Fig. 4. The boxes labeled "Yaw Model" and "Yaw Plant" are the transfer function described by (1). The only difference is that they have different $C_{\alpha h}$ parameters. The section labeled "Yaw Rate Controller" is the controllers described by (5) and (6).

By closing the yaw rate control loop with the feedback and the feed-forward controllers, the closed loop yaw rate transfer function is (9).

$$G_{r_{CL}} = \frac{(k_{pr} + k_{ff}K)G_{Pr}}{1 + k_{pr}G_{Pr}} \tag{9}$$

The differential equation of the closed-loop yaw rate is represented by (10) where the n_i and d_i coefficients are from (1).

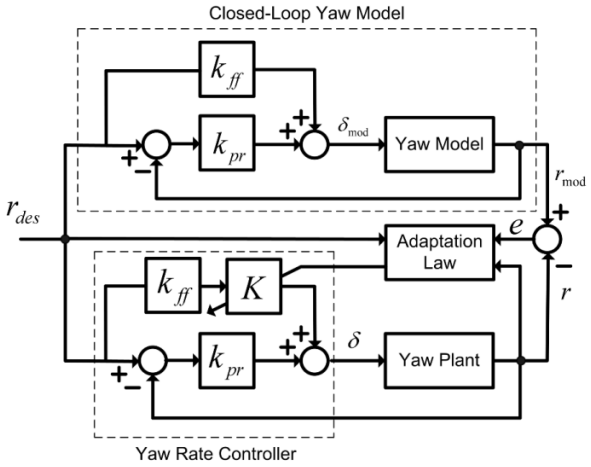

Fig. 4. MRAC for Yaw Rate Controller

$$\begin{aligned} r &= \eta(\lambda n_1 \dot{r}_{des} + \lambda n_0 r_{des} - \mu r - \rho \dot{r} - d_2 \ddot{r}) \\ \eta &= \tfrac{1}{d_0 + n_0 k_{pr}} \\ \lambda &= k_{pr} + k_{ff} K \\ \mu &= d_0 + n_0 k_{pr} \\ \rho &= d_1 + n_1 k_{pr} \end{aligned} \tag{10}$$

The adaptation law is derived by minimizing the cost function of the error between the yaw rate outputs of the model and tractor. The cost function and error definition are shown in (11).

$$\begin{aligned} e &= r_{mod} - r \\ J &= \tfrac{1}{2} e^2 \end{aligned} \tag{11}$$

The MIT rule finds the equation that moves the adaptation parameter K in the direction of the negative gradient of J. Over time, K changes so that J is at a global minimum. The time rate of change of the adaptation parameter K that is represented by (12) that minimizes (11).

$$\frac{dK}{dt} = -\gamma \frac{\partial J}{\partial K} = -\gamma e \frac{\partial e}{\partial K} = \gamma e \frac{\partial r}{\partial K} \tag{12}$$

The time rate of change of K is essentially an adaptation gain γ times the negative gradient of r with respect to K times the adaptation error e.

By applying the previous equations to (10), the adaptation law is defined by (13).

$$\tfrac{dK}{dt} = \gamma \tfrac{k_{ff}}{d_0 + n_0 k_{pr}} (n_1 \dot{r_{des}} + n_0 r_{des}) \cdot e \tag{13}$$

Though some of the parameters in this equation are not known explicitly, they can be approximated by using the same $C_{\alpha h}$ parameter as the model or absorbed into the adaptation gain γ. All that has to be known exactly is the sign of the parameters, and this is known since the sign of $C_{\alpha h}$ is always positive.

TABLE I

STEERING ACTUATOR PARAMETERS

Parameter	Value
ω_n	28.425rad/s
ζ	0.633

TABLE II

STEERING ACTUATOR SATURATION PARAMETERS

Parameter	Value
δ_{max}	32deg
$\dot{\delta}_{max}$	20.6deg/s

IV. MRAC MODIFICATIONS

A. Actuator Dynamics

Through simulations, it was discovered that the algorithm would not converge due to neglected steering actuator dynamics and saturations. A new algorithm could be derived including the inner-loop steering dynamics, but higher order derivatives of the yaw rate are needed. This is not practical since higher order derivatives are not measurable and numerical differentiation in extremely noisy. Therefore, the adaptation algorithm derived assuming infinitely fast steering actuator dynamics are used, and the actual dynamics and saturations are included into the reference model. This allows the yaw rate output of the model to behave like the actual tractor yaw rate. Simulated and experimental results will show that this approximation will be a good solution for this problem.

Previous research has been completed on identifying the steering actuator parameters [1]. The steering actuator can be modeled as a second order system with an integrator as seen in (14) where the identified parameters are listed in Table I.

$$G_{P\delta} = \frac{\delta(s)}{\delta_{input}(s)} = \frac{\omega_n^2}{s(s^2 + 2\zeta\omega_n \cdot s + \omega_n^2)} \tag{14}$$

Fig. 5 shows that block diagram that will replace the box labeled "Closed-Loop Yaw Model" in Fig. 4. As can be seen, the inner loop steering dynamics have been added to the reference model.

B. Actuator Saturations

The steering actuator saturations are then added to the reference model in the same way that the dynamics were added. The steering actuator can only turn the front wheels to a certain angle, δ_{max}, and after which the steering angle is saturated. This restriction will be added into the reference model as depicted in (15).

$$\delta_{mod_{max}} = \delta_{max} \tag{15}$$

In the same way that the steering angle can be saturated, the steering actuator can only turn the front wheels at a maximum slew rate of $\dot{\delta}_{max}$. Thereafter, the steering actuator is saturated. The slew rate of the model steering actuator will follow (16).

$$\dot{\delta}_{mod_{max}} = \dot{\delta}_{max} \tag{16}$$

The saturation properties of the steering actuator are listed in Table II.

During periods when the steering actuator is saturated, the gradient of the cost function defined in (12) and (13) become invalid. During typical operation, periods when the steering actuator is saturated are brief; therefore, the adaptation will follow the relationship depicted in (17).

$$\frac{dK}{dt} = \begin{cases} \frac{dK}{dt} & \text{for} \quad |\dot{\delta}_{meas}| < \dot{\delta}_{max} \quad |\delta_{meas}| < \delta_{max} \\ 0 & \text{for} \quad |\dot{\delta}_{meas}| \geq \dot{\delta}_{max} \quad |\delta_{meas}| \geq \delta_{max} \end{cases} \tag{17}$$

V. SIMULATED AND EXPERIMENTAL RESULTS

A. Simulated Results

In previous studies, it has been shown that $C_{\alpha h}$ can range between 0 N/deg and 4000 N/deg [8]. It is desired that the adaptation gain K have the value of 1 in the middle of the DC gain range. A plot of the DC gain verses $C_{\alpha h}$ at $V_x = 2$ m/s is shown in Fig. 6. From this plot, it can be seen that $C_{\alpha h} = 600$ N/deg puts the DC gain in the middle of the range. This allows the controller to be nominally tuned for a middle of the range implement. K will go up for a heavier implement and will go down for lighter implements.

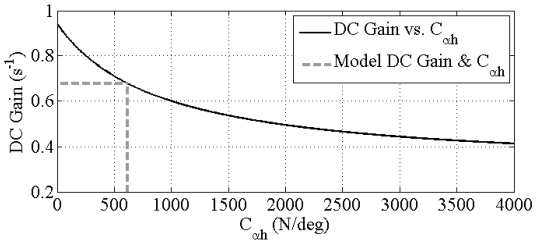

Fig. 6. DC Gain verses $C_{\alpha h}$ for the Bicycle Model with Augmented Hitch Force with $V_x = 2$m/s

A simulation of the system was performed in MATLAB to test the performance of the algorithm. All measurements were assumed to be noise and bias free. Table III lists the parameters used in the simulation. The tractor and model yaw rate plants were simulated using all of the same parameters with the exception of $C_{\alpha h}$. The simulation was conducted using a cosine yaw rate reference signal to provide enough excitation and allow the steering actuator to be initially saturated.

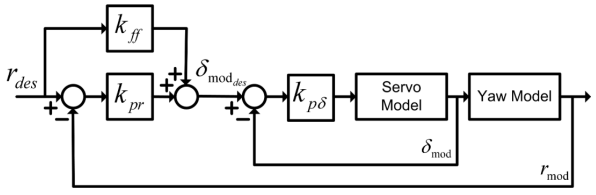

Fig. 5. MRAC Desired Closed-Loop Model with Steering Actuator Dynamics

TABLE III

TRACTOR MODEL PARAMETERS

Parameter	Value
a	1.00m
b	2.00m
c	2.19m
I_{zz}	18500kg $\cdot$ m^2
m	11340kg
$C_{\alpha f}$	2400N/deg
$C_{\alpha r}$	5000N/deg
$C_{\alpha h,mod}$	600N/deg
$C_{\alpha h,trac}$	1500N/deg
V_x	2m/s
k_{pr}	0.30
$k_{p\delta}$	3.84

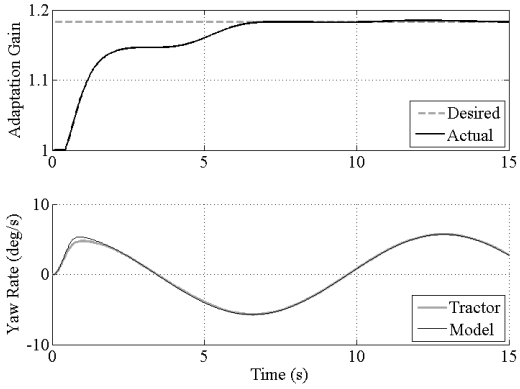

Fig. 7. Simulated Adaptation Gain & Yaw Rate Response

The adaptation gain K and yaw rate response is shown in Fig. 7. The desired K that allows the adaptation error to go to zero is calculated by dividing the DC gain of the model by the DC gain of the tractor as seen in (18).

$$K_{des} = \frac{K_{DC_{model}}}{K_{DC_{trac}}} \tag{18}$$

As can be seen in the adaptation gain response, K is constant for the first second while the steering actuator slew rate is saturated as seen in Fig. 8. Once the actuator becomes unsaturated, the gain converges to its true value. The yaw rate response shows that the model and the tractor yaw rate outputs converge to the same value once the gain reached its desired value. This shows that the algorithm works in making the tractor's yaw rate output match the model's output. Notice in Fig. 8 that the steering angle of the tractor exceeds the value of the model. This shows that the DC gain of the tractor is less than the model, and more steering angle is required to produce the same amount of yaw rate as the model.

B. Experimental Results

The algorithm was next implemented on a John Deere 8420 farm tractor. A signal is sent to the steering valve to command the flow rate at 50 Hz. To combat gyroscopic sensor noise, a second order 5 Hz Butterworth filter was implemented on the yaw rate measurement.

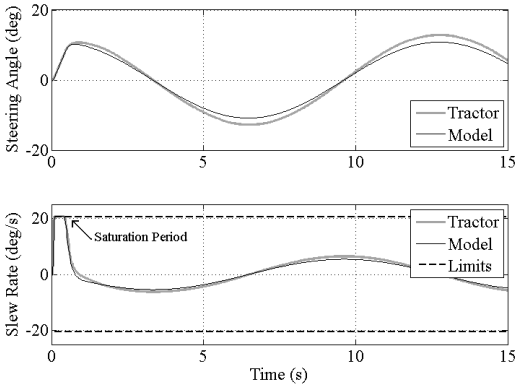

Fig. 8. Simulated Steering Actuator Response

The desired path for each experiment is a straight line. For the first set of experiments, the tractor was started off the desired path by $y_{err} \approx 2.0$ m and $V_x \approx 2.0$ m/s. The step response of the lateral position can be seen in Fig. 9. The left plot is with a four-shank ripper, and the right plot is with no implement. The adaptation gain and the yaw rate response is shown in Fig. 10, and steering actuator response is shown in Fig. 11. Notice that the steering actuator slew rate is initially saturated as it was in the simulation. The adaptation gain is held constant during this period, and it is allowed to adapt when the saturation stops. The adaptation gain reaches approximately the desired value in both experiments. The desired adaptation gain was found by system identification tests to estimate the DC gain of the tractor with and without an implement. This shows that the algorithm finds the approximate gain to match the tractor yaw rate reference model yaw rate. Once the tractor gets on the line, there is not enough persistence of excitation for the adaptation gain to converge to the exact desired value since the yaw rate is approximately equal to zero.

The next experiment presented is several runs with and without the adaptation algorithm implemented on-line. Experiment A consisted of seven runs with the four-shank ripper and the adaptive control working on-line. Experiment B consisted of seven runs with the four-shank ripper and no adaptation. Experiment C consisted of seven runs with no implement and on-line adaptation, and experiment D consisted of seven runs with no implement and no adaptation. For all runs, the tractor was traveling at $V_x \approx 2.0$. Each run

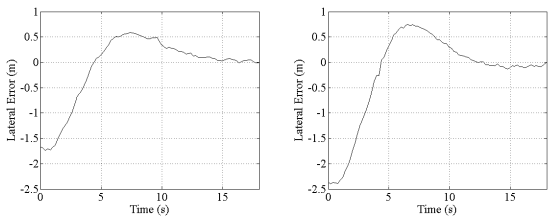

Fig. 9. Experimental Lateral Error Response (Left Column: 4 Shank Ripper; Right Column: No Implement)

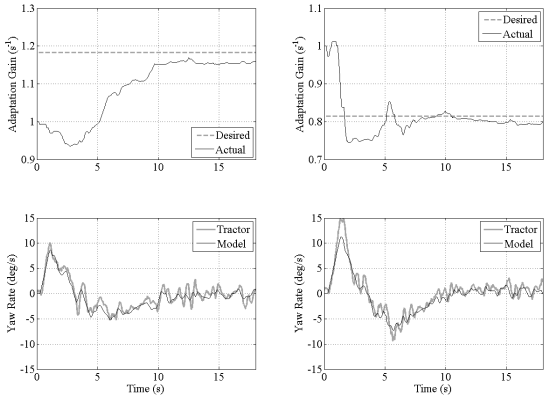

Fig. 10. Experimental Adaptation Gain & Yaw Rate Response (Left Column: 4 Shank Ripper; Right Column: No Implement)

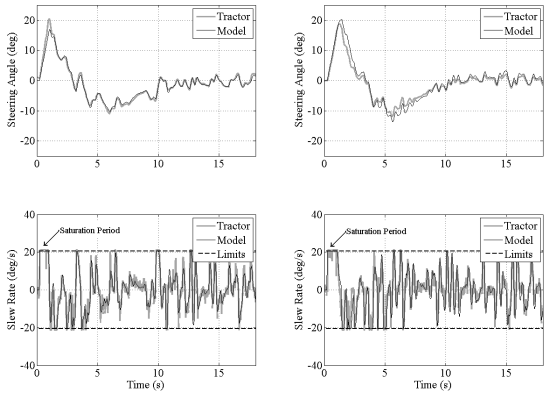

Fig. 11. Experimental Steering Actuator Response (Left Column: 4 Shank Ripper; Right Column: No Implement)

is approximately 50 seconds, and only the steady state data is used for the lateral error statistics. For the runs with no adaptation, the adaptation gain was held at $K = 1$. As can be seen in Table IV, the average standard deviation of the lateral error with an implement and on-line adaptation is 13.28% less that the runs with no adaptation. Also, the average standard deviation of the lateral error with no implement and on-line adaptation is 12.81% less that the runs with no adaptation. It can be seen that the tracking performance of the tractor is modestly improved verses using a fixed-gain controller. It can also be seen in Table IV that the average gain approaches the desired value as seen in Fig. 10. There is not enough persistence of excitation from the step inputs for the gain to always reach the desired value.

VI. Conclusions and Future Works

A. Conclusions

A model reference adaptive steering control system has been developed to improve the tracking performance of an automatically steered farm tractor. The MIT rule was used to derive a controller update law to adapt to changing hitch loading. The algorithm was next modified to include inner-loop steering dynamics and saturations. Simulated results were provided demonstrating that the algorithm correctly adapts to the desired gain and show that the tractor and model outputs converge to the same value. Experimental results demonstrated improved tracking performance of the tractor.

TABLE IV

Experimental Statistics of Lateral Error and Adaptation Gain

Experiment	$\overline{x}$ (m)	σ (m)	Adaptation Gain
A	0.011794	0.052830	1.128618
B	0.017392	0.059847	1.0
C	0.022413	0.053214	0.878633
D	0.027635	0.060031	1.0

B. Future Works

There is still room for improvement for the algorithm. Yaw rate sensors have a bias that corrupts the estimation of the adaptation gain. A method for estimating this bias would be advantageous for the algorithm. A method for adapting during periods of saturations would also improve the algorithm since these periods contain a good deal of excitation.

VII. Acknowledgements

The authors greatly appreciate Deere & Company's support of this research including the use of a John Deere 8420 tractor and a Starfire DGPS receiver. Special thanks to Greg Pate of the E.V. Smith Research Center for accommodating the experimental testing of this research. Also, thanks goes to Dr. Randy Raper of the USDA National Soil Dynamics Laboratory for the use of an implement.

References

[1] E. Gartley and D. Bevly, "On-line adaptive control of a farm tractor by compensations of parameter variations," in *Proceedings of the IMECE Conference, Orlando, FL*, 2005.

[2] A. Rekow, "System identification, adaptive control and formation driving of farm tractors," Ph.D. dissertation, Department of Aeronoutics and Astronautics, Stanford University, March 2001.

[3] K. Astrom and B. Wittenmark, *Adaptive Control*, 2nd ed. Addison Wesley, Reading, MA, 1995.

[4] T. Fukao, "Active steering systems based on model reference adaptive nonlinear control," in *Proceedings of the IEEE Intelligent Transproation Systems Conference, Oakland, CA*, August 2001.

[5] T. Hessburg, "Model reference adaptive fuzzy logic control for vehicle guidance," in *Proceedings of the American Control Conference, Seattle, WA*, June 1995.

[6] S. Baslamish, "Gain scheduled active steering control based on a parametric bicycle model," in *Proceedings of the IEEE Intelligent Vehicles Symposium*, June 2007.

[7] M. O'Conner, "Carrier-phase differential gps for automatic control of land vehicles," Ph.D. dissertation, Department of Aeronautics and Astronautics, Stanford University, December 1997.

[8] P. Pearson and D. Bevly, "Comparison of analytical and empirical models to capture variations in off road vehicle dynamics," in *Proceedings of the IMECE Conference, Orlando, FL*, 2005.

[9] T. D. Gillespie, *Fundamentals of Vehicle Dynamics*. Society of Automotive Engineers, Warrendale, PA, 1992.

[10] I. Mareels, "Global stability for an mit rule adaptive control algorithm," in *Proceedings of the 28th Conference on Decision and Control*, December 1989.